Journal of Environmental Management 408 (2026) 129892

Contents lists available at ScienceDirect

Journal of Environmental Management

journal homepage: www.elsevier.com/locate/jenvman

Research article

Flood risk to population in Italy: a synoptic overview based on fatality data

Paola Salvati [a,*], Mina Yazdani [b,c], Cinzia Bianchi [a], Mauro Rossi [a]

[a] CNR IRPI, National Research Council Research Institute for Geo-Hydrological Protection, Via Della Madonna Alta 126, Perugia, 06128, Italy
[b] KWR, Water Research Institute, Nieuwegein, the Netherlands
[c] Soil Physics and Land Management, Wageningen University & Research, Wageningen, the Netherlands

ARTICLE INFO

Keywords:
Flood
Fatalities
Societal risk
Scenario
Return period
Sparse data
Italy

ABSTRACT

Floods continue to pose a threat to human life despite the major advances in managing flood risk. To quantitatively assess potential loss of life, we present a statistical approach to model societal flood risk from sparse, point information on fatal floods in Italy. At this end, the Zipf distribution and its parameters were estimated over a regular grid covering the national territory. Despite the difficulties in modelling sparse data, we tested the approach using a detailed record of 667 fatal floods at 652 different sites for 345 major or minor meteorological events during the 78-year period 1946-September 2023. The results provide new insights into the spatial variability of societal flood risk across the national territory and into the expected return periods associated with different numbers of fatalities. Model validation indicates a slight decrease in the return periods of fatal floods in the validation dataset. This suggests a possible increase in the frequency of localized events, such as flash floods or high-volume torrential floods causing at least one fatality, potentially linked to changes in rainfall regimes rather than to urbanization. The findings can contribute to refining institutional flood-risk zoning and to supporting mitigation strategies aimed at reducing loss of life. The proposed framework may also be applied to other countries where sufficiently detailed information on fatal flood events is available.

1. Introduction

Floods are a widespread hazard with significant societal and economic consequences worldwide (CRED and UNDRR, 2021). Despite major advances in flood risk management, floods continue to pose a threat to human life and health (Papagiannaki et al., 2022). Identifying the drivers that increase flood risk to the population is therefore crucial for developing effective governance frameworks and enhancing societal resilience (Wang et al., 2022), particularly as exposure to flooding is expected to triple by 2050 due to increasing population and economic assets in flood-prone areas (Merz et al., 2021). This need is highlighted by the frequent occurrence of catastrophic floods, such as the 2025 Texas flash flood, as well as by recent events in Italy, including the Emilia-Romagna flood in May 2023 (Cremonini et al., 2024; Arrighi and Domeneghetti, 2024). In addition to such extreme events, more frequent but less severe floods also contribute significantly to societal risk (Salvati et al., 2012). Reducing the loss of life and the number of people affected by natural disasters, including geo-hydrological hazards, is a key objective of the Sendai Framework for Disaster Risk Reduction 2015–2030 (UNISDR, 2015). When loss of life is the focus, risk analysis seeks to estimate the probability that a hazardous event will cause fatalities. Fatalities provide a direct quantitative measure of event intensity and can therefore support the assessment of both individual and societal risk (Cruden, 1997; Fell and Hartford, 1997; Baecher et al., 2015; Strouth and McDougall, 2021). Societal risk expresses the relationship between the frequency of hazardous events and the severity of their consequences, usually through F–N curves and captures the potential for multiple fatalities from a single event (Ball and Floyd, 1998; Baecher et al., 2015). It therefore provides a basis for defining acceptable or tolerable risk levels and risk-informed decision-making (Evans and Verlander, 1997; Reid, 2000; Sui et al., 2020;Sim et al., 2022). Over the past decades, societal risk assessment has evolved from conceptual and regulatory formulations to increasingly quantitative, hazard-specific, and decision-oriented applications. Foundational contributions by Fell and Hartford (1997), and Ball and Floyd (1998), later expanded by Fell et al. (2005), defined individual and societal risk, introduced acceptable and tolerable criteria, and formalized the use of F–N curves. These concepts were later translated into operational guidance, particularly for industrial facilities (HSE 2001), dam safety (ANCOLD, 2003; USBR, 2003, 2011; FERC, 2016), for landslide (AGS,

* Corresponding author.
E-mail addresses: paola.salvati@cnr.it (P. Salvati), mina.yazdani@kwrwater.nl (M. Yazdani), cinzia.bianchi@cnr.it (C. Bianchi), mauro-rossi@cnr.it (M. Rossi).

https://doi.org/10.1016/j.jenvman.2026.129892
Received 19 December 2025; Received in revised form 18 April 2026; Accepted 5 May 2026
Available online 20 May 2026

2007a) while Saw et al. (2009) consolidated a broader multi-hazard perspective. A major step forward was the shift from general criteria to quantitative life-loss estimation and population-based assessment. In Italy, Guzzetti et al. (2005) and Salvati et al. (2010) used historical fatality data to quantify risk to exposed populations at national and regional scales for both landslide and flood hazards. In the flood domain, Jonkman et al. (2024, 2011, 2016), Jongejan et al. (2010); Maaskant et al. (2010), and de Bruijn et al. (2014) developed increasingly advanced methods for estimating societal flood risk, demonstrating their relevance for Dutch flood safety policy and delta-scale management; Tang et al. (2021) extended these approaches to scenario-based urban flood applications in China.

Societal risk approaches are most developed for landslides. Key advances include their incorporation into land-use planning and regulation (AGS, 2007b; Porter and Morgenstern, 2013), refinement of acceptable and tolerable criteria (Macciotta and Lefsrud, 2018; Sim et al., 2022), application of F–N curves and quantitative risk assessment in case studies (Wang et al., 2022; Winter and Wong, 2020), explicit treatment of uncertainty in practical calculations (Macciotta et al., 2019), and predictive spatial modelling of societal risk (Rossi et al., 2019). Recent reviews synthesized the field and clarified the relationship between individual and societal risk in landslide analysis (Strouth and McDougall, 2021, 2022). Overall, the literature shows a shift from a mainly conceptual and regulatory notion to a quantitative, multi-hazard, and policy-relevant framework for life-safety assessment. Within geo-hydrological hazards, this framework is now well established for landslides, whereas flood applications, despite important methodological advances, remain relatively limited. Most flood risk assessments are still based on the hazard–exposure–vulnerability framework and are commonly expressed in terms of return periods (e.g. Schanze et al., 2007; Merz et al., 2010, 2014; Winsemius et al., 2013; Arnell and Gosling 2016; Wing et al., 2018; Kundzewicz et al., 2019; Li et al., 2023; Zhang et al., 2021; Tabasi et al., 2025). These approaches have led to significant advances in identifying flood-prone areas and understanding and modelling flood hazards and risks from the local to the global scale. However, they often rely on hazard maps and may not fully capture the probability and consequences of flood events in terms of loss of life. This limitation is particularly relevant where hazard information is incomplete. In Italy, for example, several fatal flood events have occurred in areas not covered by institutional hazard maps (Marchesini et al., 2021), suggesting that approaches based on observed impacts can provide valuable complementary information.

In this study, we explore the application of a societal risk approach to assess flood risk to the population using historical fatality data in Italy. The novelty of this work lies in the development of a uniform and comparable framework for evaluating societal flood risk at national scale, based on sparse but systematically collected fatality data. The method provides statistical indicators that allow the ranking of areas according to the expected number of fatalities and the estimation of return periods associated with fatal flood events. Unlike traditional approaches based on predefined return periods, the proposed framework derives return periods as a function of event magnitude. Finally, to strengthen the robustness of the approach, we perform an independent validation of the model. The aim of the study is to provide a comprehensive and spatially consistent overview of societal flood risk in Italy and to generate geographically distributed risk scenarios based on the expected number of fatalities.

2. Data and methods

Fig. 1 shows the sequence of steps and processes, along with their outputs, used to model, validate and represent societal flood risk levels across Italy. The analysis is based on a spatially distributed statistical framework that employs the Zipf distribution (Zipf, 1949) to model the frequency–magnitude relationship of fatal flood events. The approach is applied over a regular grid covering the Italian territory using a dataset of historical flood fatalities. The methodology builds on previous applications of the Zipf distribution to landslide risk (Rossi et al., 2019) and is supported by evidence that floods and landslides exhibit similar frequency–magnitude behaviour, while they differ significantly from those associated with earthquakes and volcanic events (Salvati et al., 2012). Both geo-hydrological hazards are typically triggered by intense rainfall and are influenced by comparable environmental conditions. On this basis, we assume that the same statistical framework can be applied to flood fatalities.

The georeferenced catalogue of flood fatalities (1946–2023 sept.) is first analysed in relation to CORINE Land Cover (CLC) to verify that the distribution of fatal floods was not concentrated in urban and

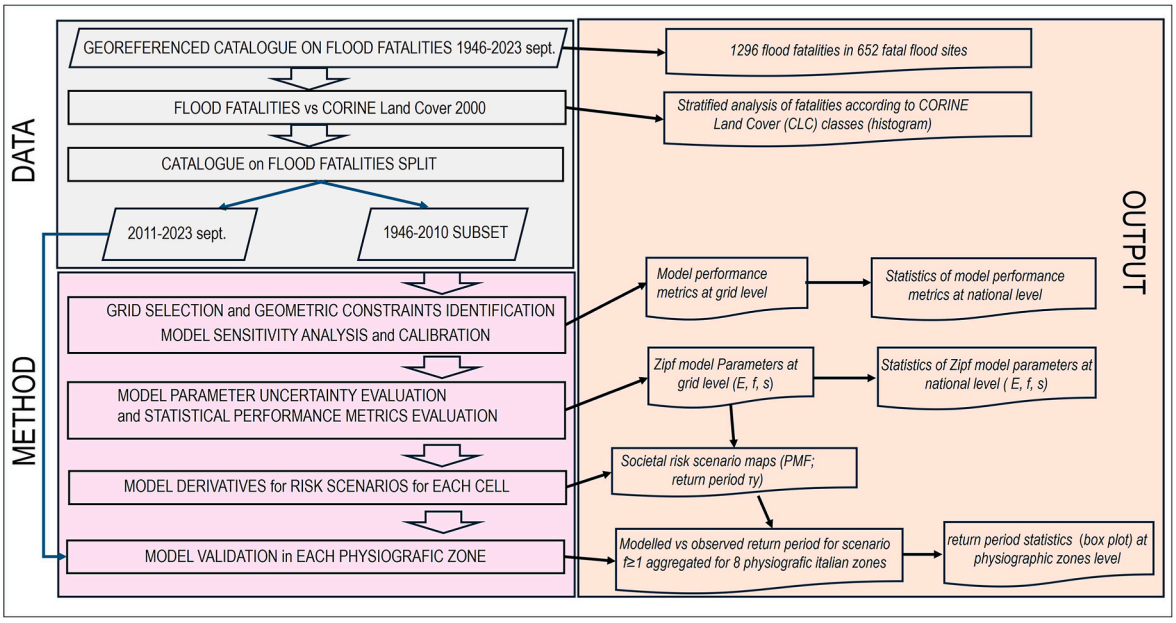

Fig. 1. Workflow of the methodological framework adopted to estimate societal flood risk in Italy. The scheme summarises the input data, analytical steps, and model outputs, including the split of the flood-fatality database, model calibration and validation, estimation of the Zipf distribution parameters, and the generation of societal flood-risk scenarios and return-period maps at the national scale.

anthropised areas compared to rural and forested areas. The dataset is then divided into training and validation subsets. A moving-kernel approach over a regular grid is used to estimate the parameters of the Zipf distribution and to perform model calibration, sensitivity analysis, and uncertainty evaluation. The calibrated model is then used to derive societal risk scenarios for each grid cell and to produce national-scale maps of potential fatal floods and their associated return periods. Model performance and validation are assessed at both grid and physiographic-zone scales.

2.1. Data on flood fatalities

Salvati et al. (2018, 2010) have consistently compiled and updated the Italian catalogue of historical floods with direct human consequences on the population, including deaths, missing persons, injured people, homeless and evacuees. Data are available on different open platforms (https://osf.io/sm8tv/files/osfstorage) and the most recent ones are annually published in the periodic report on flood and landslide fatalities on https://polaris.irpi.cnr.it/. The procedures used and the challenges encountered in compiling the catalogue are described in Guzzetti et al. (2005) and Salvati et al. (2010, 2018). In this study, we have used the updated catalogue for the period 1946–September 2023. The geographical distribution of the fatal flood events is shown in Fig. 2a with respect to the regional administrative subdivisions of the Italian territory (Fig. 2b) and the eight major physiographic/morphological zones established by Guzzetti and Reichenbach (1994) (Fig. 2c). (The list of acronyms and abbreviations is provided in full in the §1 Supplementary Materials).

Cumulatively, in the 78-year period 1946 -September 2023, 1269 people lost their lives due to 667 fatal flood events at 652 different sites for 345 major or minor meteorological events (Triggers) that caused one or more floods. This is an average of 8.5 fatal floods and 16.3 flood fatalities per year. For four of the 78 years in the record (5.1%) no fatal events were registered. The various resources used to obtain information allow us to determine the exact locations where a river breached its levees, overflowed, and inundated roads or ground floors of buildings, especially for more recent events. Therefore, it is possible to assign the exact number of fatalities caused by a single flood phenomenon at different locations. Fatal floods are relatively widespread across Italy, although more critical areas can be identified, particularly in the narrow valleys of the Alpine mountain chain that borders Italy to the north (1—Alps in Fig. 2c) and along the hilly and mountainous Tyrrhenian coast (3—AlAp, 4—Apen, 5—Tyrr in Fig. 2c).

To analyse the geographical distribution of fatal events in relation to land use, we performed a stratified analysis based on the CORINE Land Cover 2000 (CLC2000) dataset provided by the European Environment Agency (EEA, 2000). This analysis aimed to verify whether the spatial distribution of fatal floods appears strongly influenced by land-use patterns or by the presence of urbanised areas, and to assess whether a clear imbalance exists between fatal floods occurring in urban and

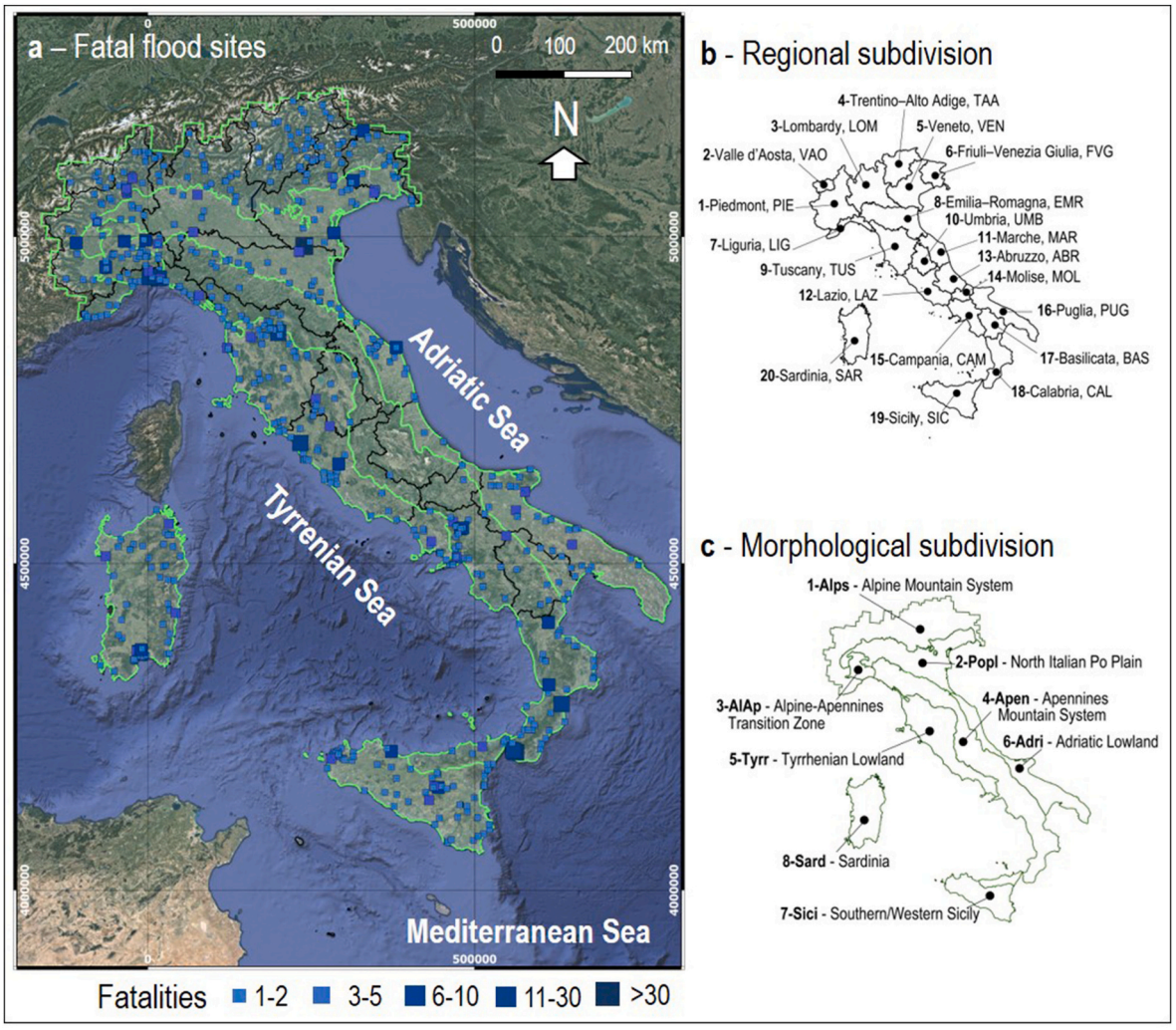

Fig. 2. Geographical distribution of fatal floods in Italy during the 78-year period 1946–September 2023. Event magnitude is expressed by the number of fatalities, represented by blue squares of increasing size and colour intensity. (b) Regional administrative subdivision and (c) morphological subdivision of the Italian territory.

rural areas. The CORINE Land Cover classification includes 44 land-cover classes organised within a three-level hierarchical structure.

The histogram in Fig. 3a shows the number of fatal flood events classified according to CORINE Land Cover (CLC) Level 3 classes, while the map in Fig. 3b illustrates their geographical distribution, with flood sites coloured according to the same CLC categories. This map reveals that the fatal floods predominantly occurred in agricultural (dots in yellow to orange), forest (dots in green), and water body areas (dots in light blue). The geographical distribution of fatal floods in continuous (CLC 1.1.1) or discontinuous (CLC 1.1.2) urban fabric (red dots) indicates that these events mainly occur in urbanised areas along the coasts, particularly along the Tyrrhenian coast. The histogram in Fig. 3c presents the data aggregated by the five Level 1 CLC classes. Fatal floods occurred in territories classified as agricultural (yellow bar, n.301, 45%; accounting for 590 fatalities, 40.2%), forest (green bar, n.121, 18.1%; accounting for 210 fatalities, 14.3%), and water body areas (light blue bar, n.12, 1.8%; accounting for 17 fatalities, 1.2%), together account for about 65% of the total fatal floods. The remaining 35% occurred in urban areas classified as artificial surfaces (red bar, n.233; accounting for 535 fatalities, 36%). Finally, Fig. 3d, shows that the average number of fatalities per flood event is very similar across the five Level 1 CLC classes. This pattern suggests that fatal flood events are not strongly concentrated in either urbanised or rural areas, although the analysis is not intended to establish causal relationships between flood fatalities and factors such as population density, infrastructure, or the presence of buildings.

2.2. The model

To estimate societal flood risk in Italy, the Zipf distribution was adopted, and the corresponding model parameters (E, F, s) were estimated across the national territory. The choice of this distribution is supported by previous studies by Salvati et al. (2010) and Rossi et al. (2019), which analysed different catalogues of fatal natural hazard events in Italy and showed that the relationship between event magnitude (number of fatalities, y-axis) and event rank (x-axis) follows an approximately linear trend in log–log space, indicating power-law behaviour.

Empirical datasets exhibiting power-law behaviour can be described using different statistical models, including the Pareto, Zeta, and Zipf distributions (Reed, 2001; Guzzetti et al., 2005; Newman, 2005; Rossi et al., 2010). The Pareto distribution describes power-law probabilities for continuous variables whose values can assume any real number above a defined minimum threshold. In contrast, the Zeta and Zipf distributions apply to discrete variables that take integer values equal to or greater than one (Reed, 2001; Newman, 2005; Friedman, 2015). The Zeta and Zipf distributions differ in their theoretical formulation: the Zeta distribution assumes an infinite population, whereas the Zipf distribution is defined for finite populations (Newman, 2005). Because the number of fatalities is inherently discrete and the maximum number of

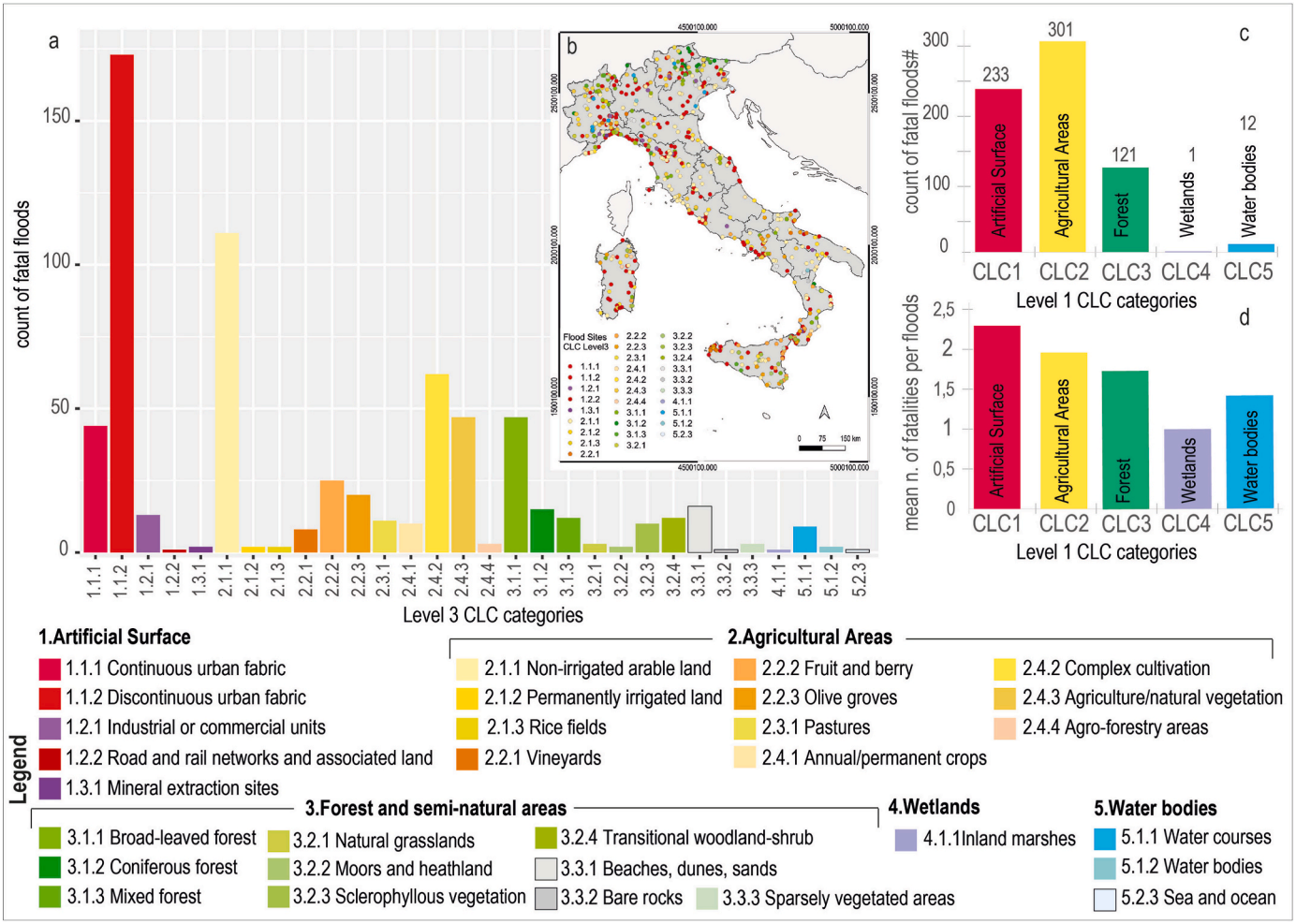

Fig. 3. Distribution of fatal flood events according to CORINE Land Cover (CLC). (a) Number of fatal floods in each CLC Level 3 class. (b) Map of fatal flood locations coloured according to the corresponding CLC classification. (c) Number of fatal floods aggregated by CLC Level 1 categories. (d) Average number of fatalities per flood event for each CLC Level 1 category.

fatalities in a single event is finite, the Zipf distribution provides an appropriate statistical framework for modelling the probability of events producing a given number of fatalities. For these reasons, the Zipf distribution has been adopted here to model the statistical behaviour of fatal flood events.

To estimate the Zipf distribution and its parameters we used the dataset of flood fatalities over the past 78 years (1946-2023 September). This data set is divided into two subsets, one from 1946 to 2010 (547 fatal events) used for the calibration of the model, and the second from 2011 to 2023 (September) (120 fatal events) for a comparison between the two periods to look for possible differences in the frequency and the return period values. The probability mass function (PMF), analogous to the probability density function (PDF) for discrete data, is expressed as:

$$\mathrm{PMF}(f; s, F) = \frac{1}{f^s \sum_{f=1}^{F} \frac{1}{f^s}} \quad \text{eq. (1)}$$

where $f \in \{1, 2, \ldots, F\}$ is the number of fatalities caused by a flood, denoting the magnitude of the fatal event. *F* represents the largest number of fatalities caused by a single fatal flood (E) in the empirical record, and $s \in R^+$ denotes the scaling exponent of the Zipf distribution model that measures the proportion of small versus large magnitude fatal events within the recorded data. Equations and description are available in the supplementary materials (§2 Equations used).

2.3. Model construction and geometric constrain

The approach involves dividing the entire Italian territory (301,340 km^2) using a regular square grid system of size *g*, in km. Subsequently, at each grid point, flood data are identified using a circular kernel with a specified radius r in kilometers. From the empirical sub-set inside the kernel of radius r, the PMF was determined adopting the Zipf distribution model. The Maximum Likelihood Estimation (MLE) approach (Clauset et al., 2009) is used to estimate the value of the s Zipf distribution parameter (White et al., 2008), and a bootstrapping re-sampling technique (Efron, 1979; Davison and Hinkley, 1997) to determine its variability (uncertainty) σ_s. Lastly, we attributed to each grid cell the three model variables $\{F_k, E_k, s_k\}$, where E_k measures the number of fatal floods in the selected sub-set, and "k" denotes values computed for the geographical sub-set of the historical record inside the kernel of size r.

To optimise the model parameters, a sensitivity analysis was performed using different kernel sizes (r = 10, 25, 40, 55, 70, 85 and 100 km) over Italy, with a fixed grid spacing of 10 km. In a kernel-based approach, the grid spacing must be sufficiently small to avoid spatial gaps; thus, the chosen value ensures continuous coverage and high spatial resolution. The 10 km spacing represents a compromise between data availability and national-scale representativeness. In addition, applied uniformly across heterogeneous settings (urban, rural, plains, and mountains), it provides a consistent spatial discretisation of the study area.

Fig. 4 summarized the results of the sensitivity analysis where the 6 plots (**a-f**) show the mean value of E (Fig. 4a) and s (Fig. 4b), the standard deviation (st.dev) of s values (Fig. 4c), the mean p-value of s values (Fig. 4d), the mean values of the 2-sided-Kolmogorov-Smirnov test (KS) p-value (Fig. 4e) and of D values (Fig. 4f) for each kernel radius. We observe an increase in the mean number of fatal floods (E) as the kernel radius increases (Fig. 4a), the same trend is present for the scaling exponent of the Zipf distribution model (*s*) (Fig. 4b), as in a larger kernel area, we expect a larger number of small magnitude floods with respect to the number of floods of higher magnitudes. For smaller sampling

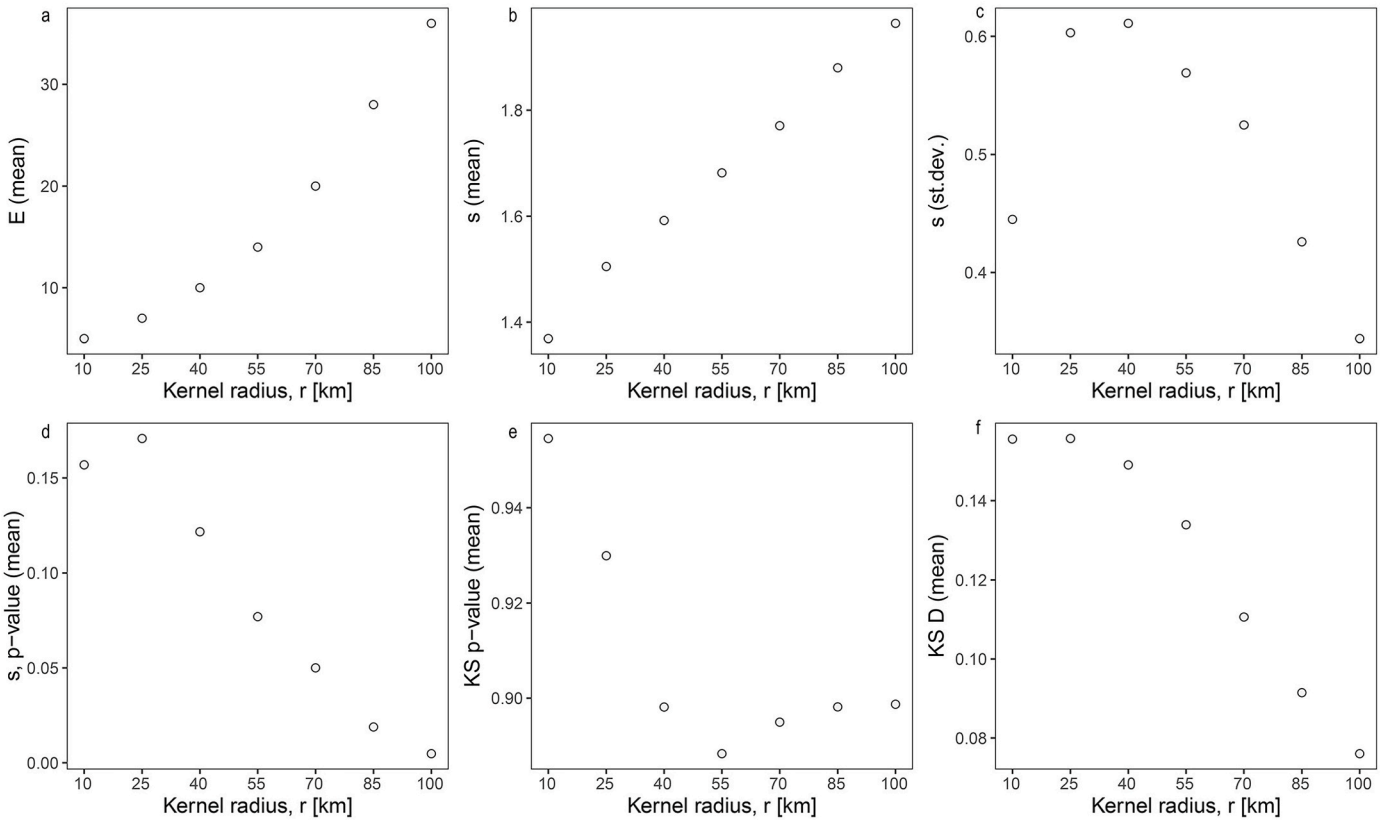

Fig. 4. Sensitivity analysis of the model with respect to the kernel radius r (x-axis, km) using a grid spacing of 10 km. Seven kernel sizes were tested (r = 10, 25, 40, 55, 70, 85, and 100 km), corresponding to kernel areas of approximately 314, 1963, 5027, 9503, 15,394, 22,698, and 31,416 km^2. For each configuration, aggregated statistics over the Italian territory were computed: (a) mean number of fatal floods (E); (b) mean value of the scaling exponent of the Zipf distribution (s); (c) standard deviation of s; (d) p-value of s; (e) mean p-value of the two-sided Kolmogorov–Smirnov test (KS); (f) mean KS D-statistic.

kernels (smaller r), the algorithm selects a small number of events and with very similar magnitude, (normally the very low magnitude events that are the most frequent) thus moving from one grid point to the other, the variability of the *s* parameter remains at a low value. This means that for smaller samples, the geographical sub-set is not large enough to describe the signal well. Enlarging the kernel up to a certain point (r = 40 km), we observe that, after the maximum value in the standard deviation of the *s* parameter σ_s (Fig. 4c), it starts to decrease (r ≥ 55 km), indicating that we are getting closer to a less uncertain estimation which is more aligned with reality. Fig. 4d depicts the mean value of the significance of s parameter (*s*, p-value in the figure) which is obtained from a Z test to verify the parameter difference from zero, where we observe significant values (*s*, p-value ≤0.05) for kernel sizes with r ≥ 70 km. This is due to a larger number of empirical data being selected in larger kernels for the estimation of the Zipf distribution models. Lastly, Fig. 4e and f indicate the results of the 2-sided Kolmogorov-Smirnov test that measure the difference between the empirical (observed) and the Zipf-modelled data for different kernel sizes, and the relative p-value. Notably, we observe that the KS p-value (Fig. 4e) starts to stabilize from a radius of 70 km onwards. This result combined with those of the s p-value (Fig. 4d) allowed us to identify 70 km as the optimal radius size. Therefore, g = 10 km and r = 70 km were chosen as the most suitable parameters to build our geographically distributed predictive model of societal flood risk in Italy. The model provides a spatial resolution of 10 × 10 km^2, and the single Zipf models are determined at each grid point using a kernel area of about 15,394 km^2 (*r* = 70 km). This means that on average at each grid point, 19 fatal floods were selected to estimate the single Zipf model parameters (Table S1 in supplementary materials provides the results).

3. Application of the model

The modelling process results in a regularly spaced estimation of the societal flood risk over Italy, represented by the three parameters (E, F, s) of the Zipf distribution. Collectively, the model results were computed for 2918 grid cells covering 97% of the Italian territory and results (Fig. 5) provide diverse, independent and complementary pictures of societal flood risk in Italy. To ensure the statistical robustness of the Zipf parameter estimation, the model was applied only to kernels containing at least six fatal flood events. Kernels with fewer events were excluded from the parameter estimation.

Fig. 5a represents results of the discrete Probability Density Function (PDF) of the largest magnitude flood (F), in shades of orange, and the corresponding Empirical Cumulative Distribution Function (ECDF), line

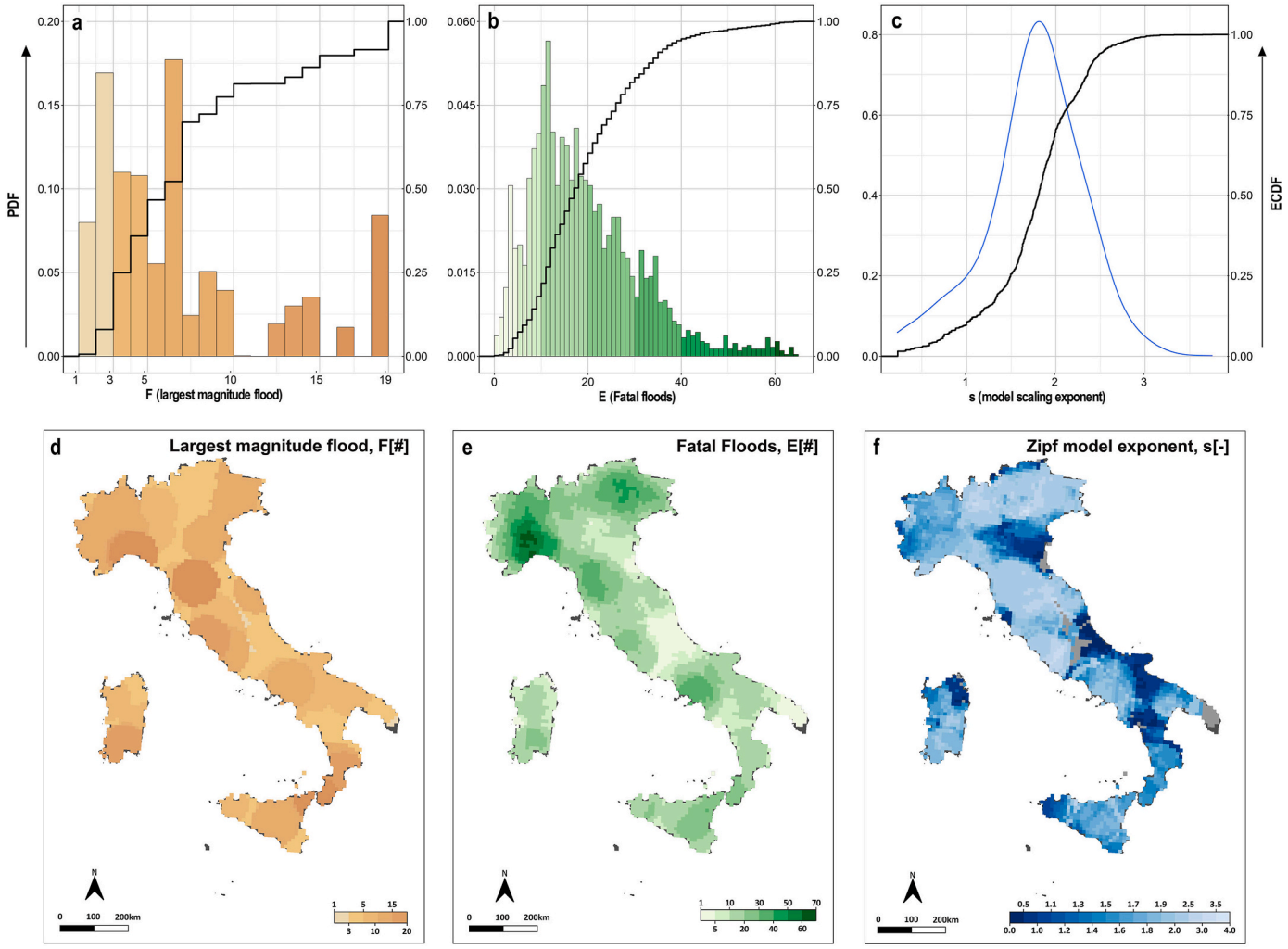

Fig. 5. Spatial distribution of the parameters of the societal flood risk model. Top row (a–c) shows histograms of the Probability Density Function (PDF; coloured bars) and the Empirical Cumulative Distribution Function (ECDF; black line). Bottom row (d–f) shows the spatial distribution of: (d) F – the largest magnitude fatal flood; (e) E – the total number of fatal floods; (f) s – the scaling exponent of the Zipf distribution model. Light grey indicates areas where the scaling exponent s was not calculated due to insufficient data, while dark grey indicates areas where no fatal flood data were available. All parameters were estimated using data from the 65-year calibration period 1946–2010. Refer to Fig, 1 for the Italian geographical and administrative subdivision.

in black. The highest probability densities are associated with flood magnitudes of 3 and 7 fatalities (with PDF values of 0.17 and 0.18, respectively), while the probability density for flood events of magnitude 8 and higher drops below 0.05, except for the largest magnitude of 19 fatalities, the highest one recorded in the study period. On the other hand, based on the ECDF graph, approximately 21% of the Italian territory experienced the largest magnitude floods of exceeding 10 fatalities ($F_k > 10$). As shown in Fig. 5b, the E distribution, illustrated in shades of green, displays a skewed pattern. The highest probability density is observed in areas that have encountered 11-12 fatal floods (PDF = 0.057). According to the ECDF, approximately 31.3 % of the Italian territory experiences a maximum of 12 fatal floods ($F_k \leq 12$). Furthermore, high numbers of fatal floods ($F_k \geq 40$) are less frequent, occurring in only 8.04% of Italy. The probability distribution of s, the scaling exponent, as illustrated in Fig. 5c, is characterized with a peak of 0.83 corresponding to $s_k = 1.8$. This indicates that 48.06 % of the national territory experiences s values $s_k \leq 1.8$. These areas are characterized by a higher prevalence of smaller magnitude floods with only a few fatalities, and a proportionally lower occurrence of larger magnitude floods. In contrast, gentler model curves ($s_k \leq 1$) were derived for 8.3% of Italy, where larger magnitude floods were more prevalent than small magnitude ones. Much steeper model curves ($s_k \geq 2.24$) are obtained for nearly 20% of the territory. These areas are indicative of a significantly higher proportion of small magnitude floods in comparison to larger-scale events. A detailed discussion of the results across the Italian territory and of Fig. 5 d, e, f, is available in the supplementary materials (**§4** Description of Zipf parameter results across Italy).

3.1. Flood risk scenarios

Starting from the Probability Mass Function (PMF, eq. (1)) of the Zipf distribution, which describes the expected probability of observing a fatal flood of a given magnitude f, it is possible to derive different statistics, useful for the analysis of societal flood risk (variables' description available in the supplementary materials). Scenarios in Fig. 6 have been selected from all the results to concisely describe flood risk, including PMF, yCCFDF - the yearly Complementary Cumulative Distribution Function which gives the annual frequency of fatal floods of given magnitude based on the length of the historical flood fatalities data (T = 65 calibration period), and the expected return period for the fatal floods, τ_{CCFDF}.

Results from the three scenarios were mapped across the entire Italian territory using a green to violet colour scale, corresponding to an increasing level of societal risk. Inspection of the 12 maps (Fig. 6) allows for a comprehensive analysis of the modelled risk. In each column, from top to bottom, the maps show the geographical distribution of the selected scenarios for increasing numbers of potential flood fatalities, i.e. f = 1, 3, 5 and 10 fatalities (from left to right). The tables below each map list the percentage of cells for the different risk levels useful to quantify the potentially affected areas under the flood risk scenarios.

Although a detailed analytical description of the results (PMF, yCCFDF, τCCFDF) is provided in the Supplementary Materials (§5, Flood risk scenarios across Italy), here we focus on one key outcome of the method: the geographical distribution of the modelled return period associated with a given event magnitude, expressed as the expected number of fatalities. The Supplementary Materials also include the full dataset and the values of the model parameters estimated within each kernel during the calibration phase (calibration-model_data rew2. xlsx).

For the lowest magnitude floods ($f = 1$) the return period τ_{yCCFDF} is always less than 50 ($\tau < 50$ years), since all of the Italian territory is coloured by shades of light green (Fig. 6i). When $f \geq 3$ (Fig. 6j), for most of the Alps (1—Alps), large parts of the Apennines range (4—Apen), the Tyrrhenian borderlands (5—Tyrr), and large parts of the two islands Sicily and Sardinia (7—Sici and 8—Sard) collectively (74.28%), the return period is less than 200 ($\tau < 200$ years).

For medium magnitude floods ($f \geq 5$), 50.42% of the modelled areas resulted in $\tau < 200$ years in the NW and NE Alpine mountains (1—Alps), in limited areas of the Tyrrenian Borderland (5—Tyrr), and in southernmost part of the Apennine (4—Apen) including territories of Calabria (18-CAL), Sicilia (19-SIC), and Sardinia (20-SAR). Conversely in a small portion (2.29%) of Lazio region (12-LAZ) the return period increased to more than 200 ($\tau > 200$ years). For large magnitude floods ($f \geq 10$), most of Italy exhibit a very large return period ($\tau_{yCCFDF} > 1000$ years, light blue colour), whereas limited portion of territories resulted in $\tau < 200$ years including Liguria (7-LIG), very localized portions of Emilia–Romagna (8-EMR), Toscana (9-TOS) and Lazio (12-LAZ), northeastern Sicily (19-SIC), southern Calabria (18-CAL) and southern Sardinia (20-SAR) in Fig. 6l. In these areas, societal flood risk should be considered high or very high.

These results, obtained for Italy, provide strong evidence supporting the potential applicability of this method—and of the estimation of return periods for fatal floods of different magnitudes—to other regions and countries with comparable territorial extent, where historical records of fatal floods and associated fatalities spanning at least fifty years are available.

3.2. Performance of the model

To test the model capability, we attempt a validation of the societal flood risk scenarios (Fig. 6) using the most recent data of the catalogue spanning the 13-year period 2011– 2023 (September) not used for the calibration of the model. In this period 120 fatal floods caused 189 fatalities in the magnitude range $1 \leq f \leq 10$, occurred at 120 sites. In particular, the risk scenario τ_{yCCFDF} for fatal floods of magnitude $f \geq 1$ (Fig. 6i) has been considered for this purpose. Therefore, with the same parameters as those employed in constructing our model (g = 10 km and r = 70 km), the τ_{yCCFDF} is calculated on the observed recent dataset. At each grid point, using the same kernel radius of 70 km, fatal events with at least 1 fatality ($f \geq 1$) are selected, and the relative annual frequency of these events and the corresponding return periods τ are estimated with respect to the 13-year period of observation.

The purpose of the comparison was twofold: to validate the model using the most recent observed data, and to verify and quantify any differences between the respective return periods (i.e., modelled and observed), with the ultimate aim of highlighting any trends in the frequency of fatal events. Consequently, we performed the comparison between the two periods across the eight Italian main morphological subdivisions (Guzzetti and Reichenbach, 1994) (Fig. 2) based on derivatives of altitude, visual interpretation of morphometric maps, and inspection of small-scale geological and structural maps. The choice of aggregating the results of the validation dataset over this morphological subdivision is made to overcome the presence of a large number of cells where the model did not perform due to lack of data on flood fatalities. We acknowledge the imbalance in the length of the two periods (calibration period: 1946-2010; validation period: 2011-2023) and in the number and geographical distribution of fatal floods in these two datasets, however, a large part of the complete and available dataset was needed to obtain the optimal model calibration parameters based on the sensitivity analysis (§3.1). A potential solution would have been extending and shifting back the calibration dataset to before 1946, but this approach was not pursued given the possible incompleteness of the older historical records.

The comparison results are shown in Fig. 7. We have utilized boxplots, as shown in Fig. 7a, where the return period τ values of fatal floods with a magnitude of at least 1 ($f \geq 1$), over the validation period are depicted on the vertical axis, divided into seven time-intervals. This categorization is based on the distribution of the τ values calculated for the validation dataset. On the horizontal axis, we have the corresponding modelled τ return periods over the calibration period (1946-2010). In this manner, for each morphological zone, the box plot illustrates the distribution of the predicted return periods in comparison to those of the validation ones. This representation allows an immediate

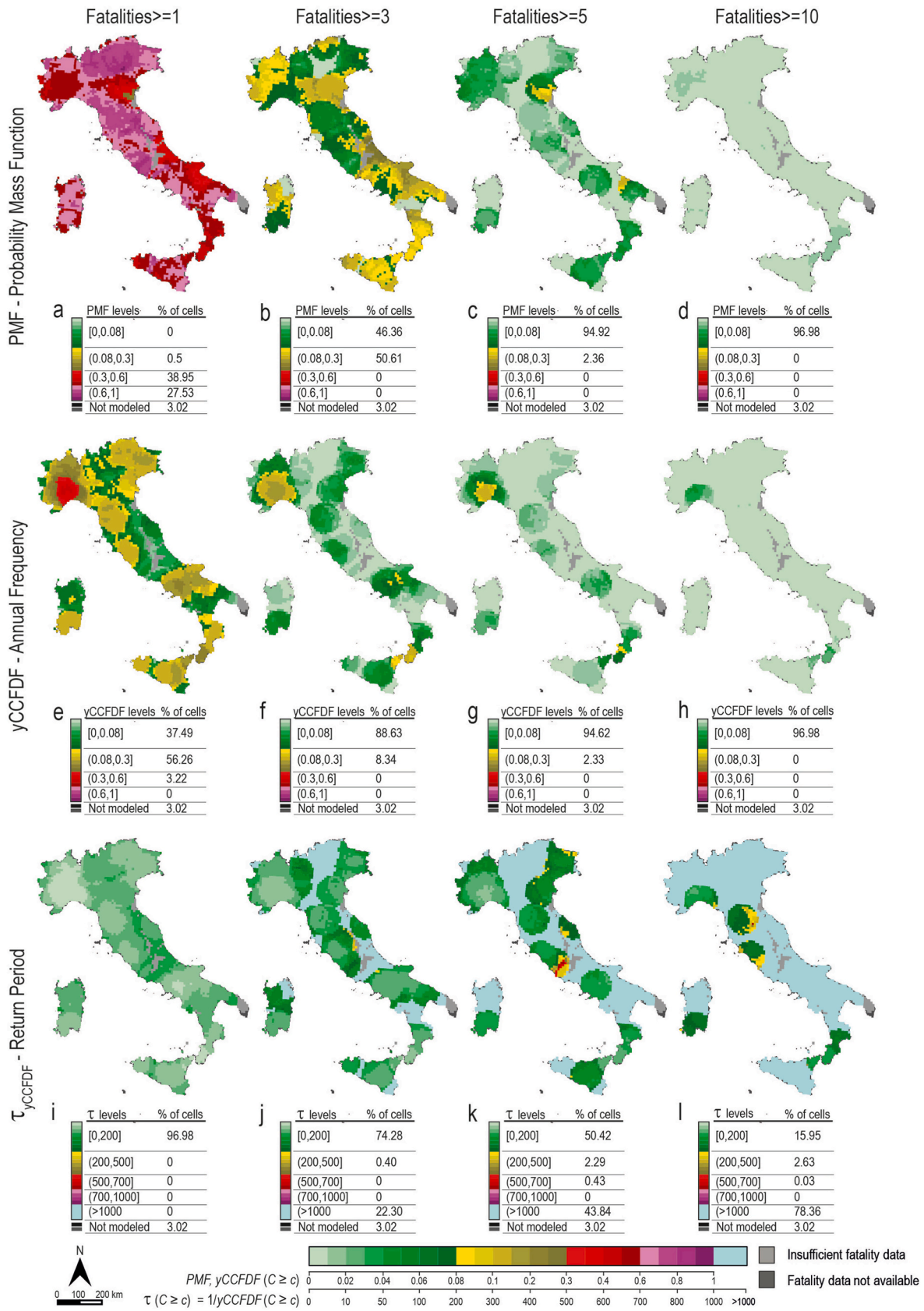

Fig. 6. Societal flood-risk scenarios for Italy derived from the Zipf distribution model. From top to bottom, maps (a–d) show the Probability Mass Function (PMF) representing the probability of fatal flood events of different magnitudes; maps (e–h) show the yearly Complementary Cumulative Distribution Function (yCCFDF), which represents the annual probability of observing flood events with at least a given number of fatalities; maps (i–l) show the expected return period of such events (τCCFDF = 1/yCCFDF). Dark grey areas indicate locations where flood-fatality data were not available, while light grey areas indicate locations where the scaling exponent *s* could not be calculated. Tables below each map report the percentage of grid cells associated with different risk levels.

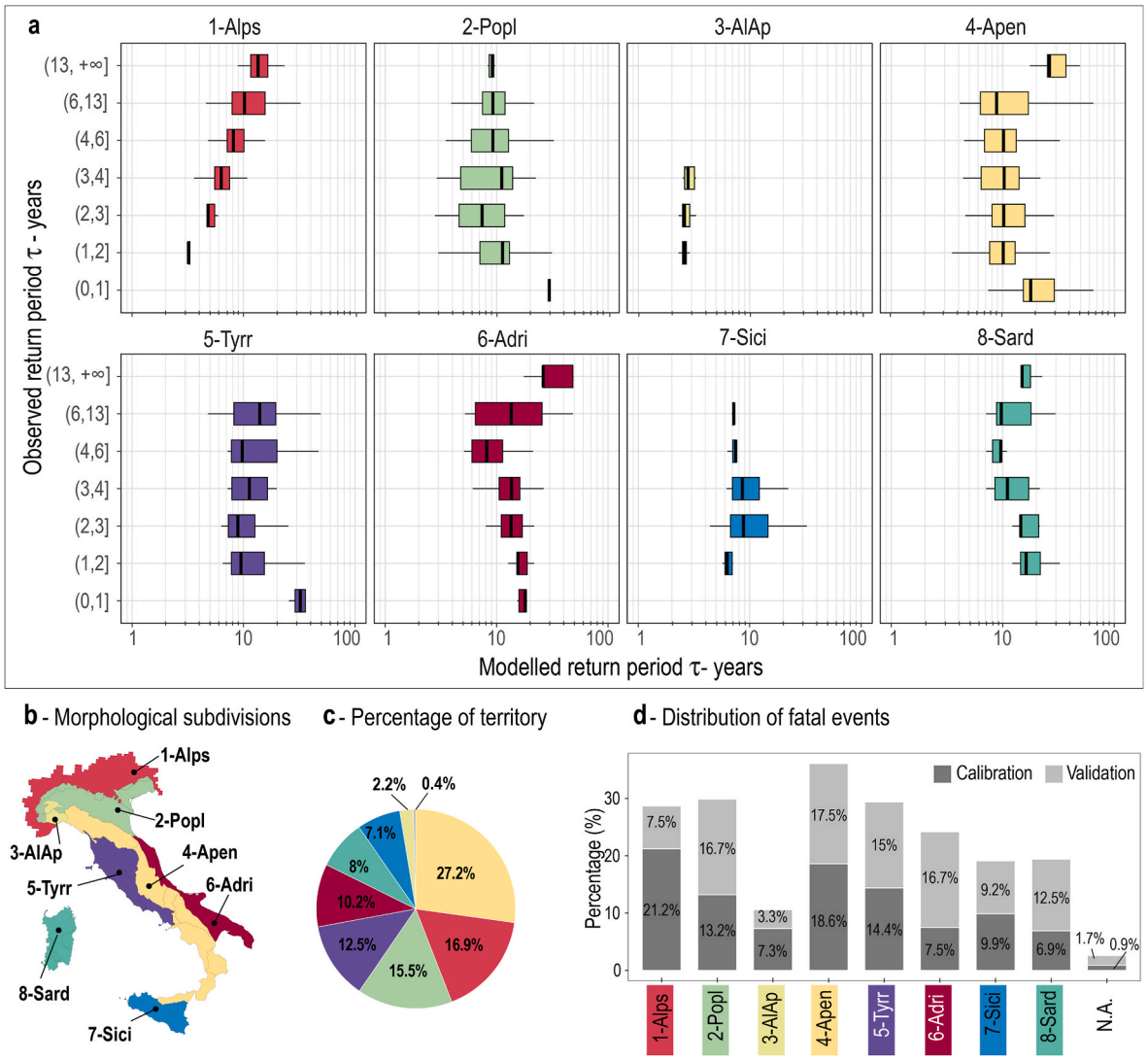

Fig. 7. Validation of the modelled return periods. (a) Comparison between modelled return periods (τ) obtained from the calibration dataset and those observed in the validation dataset (semi-log plot) across the eight main Italian morphological zones. Boxplots represent the distribution of modelled τ values corresponding to each class of observed return periods. (b) Map of the morphological zones. (c) Percentage of the Italian territory included in each morphological zone. (d) Percentage of fatal floods in the calibration and validation datasets within each morphological zone.

visualization of the performances (positive and negative) of the model applied to the risk scenarios.

Visual analysis of Fig. 7a reveals for all the morphological zones a general overestimation of the modelled return period compared to the observed one in the validation dataset. The zone that shows the best correspondence between the τ values is the 1-Alpine Mountain System zone (1—Alps). Additionally, in this zone, a clear positive correlation exists between the validation return periods and the modelled ones. A weak positive trend is also observed in the 3-Alpine-Appenine transition zone (3—AlAp), although in this area a low range of τ values are modelled and for which we do not observe τ values > 4 years. This area, covering 2.2% of the italian territory, accounts for the 7.3% of the total number of fatal floods in the calibration period and 3.3% in the comparison dataset (Fig. 7d), indicating a high fequency of occurrence for such events in such a limited area.

In 2-North Italian Po Plain (2—Popl) zone, an area which primarily consists of lowlands and that covers the wide northern Italian plains corresponding to the 15.5% of the italian territory, the behaviour is different. For the validation return periods $3 < \tau \leq 4$ years, the median of the corresponding boxplot (Median = 11 years) indicates an overestimation of the majority of the values: only those within the first quantile coincide. The model performance improves for events with larger return periods (lower frequencies) as in this zone, the model coincides with the validation values for 25% and 30% respectively for τ category of (4,6] and (6,13] years.

In 4-Apennines Mountain System zone (4—Apen), the range of the values predicted by the model for each τ category of the validation return period are much larger in comparison with the other zones. This area, corresponding to the 27.2% of all Italy, extends along almost the entire length of the national territory with a large variability in its width. It is also evident that no positive correlation exists since the median of the boxplots is almost costant except for τ = 1year. A clear signal of positive correlation is missing in the other morphological zones of 5-Tyrrehenian Lowland (5—Tyrr), 6- Adriatic Lowland (6—Adri), 7-Southern/Western Sicily (7—Sici) and 8-Sardinia (8—Sard) and the overestimation of the modelled τ compared to the observed period is persistent. Lastly, around 0.4% of area covered by the grid system have not been classified in any of the morphological zones (n.a. in Fig. 7c and d). From this comparison, we can extrapolate that the best model performance corresponds to the 1-Alpine Mountain System zone (1—Alps), where the percentage of fatal floods in the calibration dataset is the largest (Fig. 7d), and the proportion between the validation (7.5%) and

the calibration (21.2%) datasets are balanced with respect to the extent of the corresponding period (13 and 65 years respectively). On the contrary, in other zones such as the 4-Apennines Mountain System zone (4—Apen) a quite identical percentage of fatal floods is recorded within the two periods with very different lengths. This confirms that in the most recent period signals of increased frequency are present and not to be ignored.

4. Discussion

Risk estimation is inherently complex, as it requires the integration of numerous variables and typically represents the final stage of extensive analytical and modelling efforts (Merz et al., 2014). When assessing risk to the population, additional social and cultural factors must also be considered (Tabasi et al., 2025), as they play a crucial role in shaping vulnerability (e.g., Birkmann, 2007; Ciurean et al., 2013).

To develop our model of societal flood risk in Italy (Figs. 5 and 6), based on the historical record of fatal floods (Figs. 1 and 2), we assumed—while acknowledging that this represents a strong simplification—that three variables can jointly provide an informative measure of flood risk to the population: the largest magnitude of fatal floods, the total number of fatal flood events, and the scaling exponent of the Zipf distribution model.

We recognize that these assumptions may influence the resulting risk estimates. However, we consider it a reasonable compromise between a purely hazard-based framework, which requires the explicit estimation of hazard, exposure, and vulnerability components, and a risk-based approach based on frequency–magnitude relationships.

This study aims to provide a nationwide, standardized overview of the risk that floods pose to the population. The lack of homogeneous and comprehensive hazard assessments across the Italian territory, together with the limited availability of socio-economic data required to quantify exposed elements and their levels of vulnerability, motivated the adoption of this risk-based framework. A significant number of catchments, primarily smaller basins, still lack a formal assessment of flood hazard in Italy (Marchesini et al., 2021) although flood-related fatalities continue to occur in these areas.

The approach presented in this study is supported by the underlying data: a complete and standardized historical time series representing a robust sample of the population affected by flood fatalities since 1946 — (the post-World War II period in Italy) — together with the use of a rigorous statistical framework. In addition, a substantial body of scientific literature supports the applicability of societal risk criteria to natural hazards, including floods. The possibility of identifying potentially catastrophic floods with a large number of fatalities, together with their associated return periods, can provide a valuable tool for improving flood risk management.

The application of the method to the Italian territory demonstrates its applicability over large spatial domains and contributes to improving knowledge of the risk posed to the population. The results provide complementary information that supports the Flood Risk Management Plans developed in compliance with the European Floods Directive (EU, 2007).

4.1. Considerations on societal flood risk level in Italy

In this study we modelled societal flood risk based on the record of historical fatal floods that has temporal and geographical dimensions, with both dimensions characterized by sparse point measures. The geographical distribution of fatal floods (Fig. 2) and the estimated Zipf variables (Fig. 5) confirm that flood events were abundant in most of the Italian territory.

The ECDF of the E variables (Fig. 5b) show that almost 50% of the territory experienced at least 20 fatal floods during the investigated period, conversely, just over 10% of the national territory had experienced high number of fatal floods (E between 35 and 65). At the same time, nearly 50% of the country suffered from floods with $1 \leq f \leq 7$ fatalities per event (Fig. 5a–d). This confirms that, despite the high frequency of these deadly events, their magnitude, expressed in terms of the number of fatalities, is not so high. We explain these results considering the complexity and variability of the flood mechanisms (e.g. natural exceedance, defence exceedance etc.) that can occur as a consequence of the same storm (trigger) simultaneously along one or more river/stream channels affecting large areas. Consequently, the spatial distribution of the fatal floods is sparse and fragmented in multiple localities, reflecting different morphological, physiographic and anthropic settings contributing to the occurrence of fatalities. Furthermore, the likelihood that a flood will cause fatalities and, consequently, the risk level to the population is a function of many socio-economic variables that, together with the physical and hydraulic characteristics of the flood phenomenon, affect the number of fatalities that each flood may cause. First the behaviour of people can further influence whether or not the fatal condition occurs (Salvati et al., 2018; Hamilton et al., 2020; Petrucci, 2022). Secondly, the type of building, its characteristics and the presence of basements influence the number of fatalities (Diakakis and Papagiannaki, 2021). Furthermore, the alert systems and other forms of reducing risk in Italy, as at global scale (Jonkman et al., 2024), improved flood risk management practices over recent decades leading to a downward trend in the number of deaths per event.

To account for possible relations between the land use and the occurrences of fatal floods, the latter were analysed versus the land cover data from the CORINE project (2000) (Fig. 3c and d). It emerged that there is no a great difference between the average number of fatalities per event in the urbanised areas and rural and forested areas. We are aware that the time span of the historical records, used to model the societal flood risk, does not overlap with that of the CORINE Land Cover (CLC). This means that the social and industrial transformations that have taken place in some areas of the national territory may not be captured by our analysis. A broad overview of land use changes in Italy, and in particular of the relationship between land-use/land-cover changes and human population changes in Italy has been studied by Falcucci et al. (2006). The authors found that from the 1960s to 2000 in Italy forest increased, replacing mainly agricultural areas and pasture and agriculture remained mostly unchanged. Since 65% of the fatal floods occurred in rural and forested areas, (Falcucci et al., 2006), the histograms in Fig. 3 could provide an accurate representation of the distribution of fatal floods according to land use over the forty-year period. Therefore, changes in land cover did not greatly influence the geographical distribution of fatal floods. While this result supports the applicability of our method in both urbanised and rural contexts, as no significant differences were observed in the distribution of fatalities, it also raises an important issue regarding the outcomes of the validation process. If the observed increase in the frequency of local floods cannot be primarily attributed to territorial anthropisation, other potential drivers should be considered.

4.2. Validation process

The validation exercise provides an important test of the robustness of the proposed modelling framework. When comparing the return periods of fatal floods estimated by the Zipf-based model (Fig. 6) with those observed in the independent validation dataset (2011–2023), the modelled return periods appear systematically longer than those derived from the validation data (Fig. 7).

Part of this discrepancy can be explained by the different temporal length of the calibration and validation datasets. The validation dataset covers a much shorter period, which may lead to biases in the estimation of return periods based on frequency analysis. Nevertheless, the comparison highlights that fatal flood events occurred more frequently in the recent period than predicted by the model calibrated on the historical record. This discrepancy may reflect changes in the underlying conditions influencing flood impacts on the population. Although the present

modelling framework does not allow direct attribution of these changes to specific drivers such as urbanization, infrastructure characteristics, or risk perception, the results suggest that the societal risk associated with floods may have increased in recent years. This outcome represents an important result of the validation process. Rather than indicating a weakness of the modelling framework, it may suggest that the underlying conditions influencing flood impacts on the population have changed in recent decades.

One possible explanation relates to changes in precipitation regimes. Several studies have shown that, across Italy, the number of wet days has decreased while the total annual precipitation has remained relatively constant (Brunetti et al., 2001, 2004; Caporali et al., 2021; Avino et al., 2024). This pattern indicates an increase in precipitation intensity in recent decades. For landslides the increase in the frequency and intensity of severe rainfall events, a primary trigger of rapid-moving landslides causing many landslide fatalities, can be result in an increase in the number of people exposed to landslide risk (Gariano and Guzzetti, 2016). Intense rainfall events are a primary trigger for floods and are often associated with rapid hydrological responses, particularly in small mountain catchments where flash floods can occur, although there is not abundant evidence to suggest that increases in heavy rainfall would result in similar increases in streamflow (Wasko and Sharma 2017; Zhang et al., 2021). Moreover, existing scientific literature (e.g., Blöschl, 2022) highlights the considerable complexity involved in understanding how rainfall extremes, and rainfall more generally, translate into flood generation. Despite the challenge of establishing a clear connection between a specific extreme event and climate change (Pendergrass et al., 2017), which is not the focus of our work, climate projections for Europe seem to indicate a general increase in heavy rainfall with a 1-30-year return period (Tabari, 2020) as well as an increase in short-duration extreme precipitation for all return periods under both RCP4.5 and RCP8.5 (Hosseinzadehtalaei et al., 2020). Additional evidence also points evidence of future increases in hourly precipitation extremes (Kahraman et al., 2021). If these trends are already emerging, they may have contributed to an increase in the frequency of low magnitude fatal flood events (with very few fatalities).

Another possible explanation relates to the non-stationarity of the processes controlling flood impacts. If the frequency and intensity of triggering rainfall events have changed over time, the model calibrated on historical data (1946-2010) may not fully represent current conditions. The issue of non-stationarity in hazard modelling and validation is widely discussed in the literature (e.g., Kley et al., 2019).

In the present study, the limited spatial and temporal density of fatality data does not allow explicit modelling of non-stationarity effects, for example through detrending approaches (Ryan et al., 2025). To partially address this limitation, model parameter uncertainty was evaluated through resampling techniques. Despite these limitations, the validation exercise highlights an important result: fatal flood events in the recent period appear to occur more frequently than suggested by the historical record used for model calibration. This finding reinforces the relevance of continuously updating societal risk assessments as new data become available. However, we recognize the importance of collecting additional data in order to recalibrate the model using recent data representative of the current stationarity trends. Currently, recalibrating the model is neither simple nor feasible, as we cannot yet be certain that a new state of stationarity has been reached. Finally, the results of the proposed framework allow the identification of areas characterized by high expected numbers of fatalities or relatively short return periods. These areas may represent priorities for more detailed local-scale investigations, including hydraulic modelling and vulnerability assessments tailored to the appropriate spatial scale.

4.3. Societal vs social risk

It is important to note that the estimation of societal risk does not correspond to an assessment of social risk, as the two concepts refer to different analytical perspectives. While societal risk quantifies the probability of events causing multiple fatalities, social risk generally refers to the broader social consequences and vulnerabilities associated with hazardous events. These two concepts are sometimes mistakenly interpreted as equivalent concepts (Baecher et al., 2015). In addition, societal risk criteria are largely based on the concept of risk aversion, reflecting society's tendency to be more concerned about accidents (or disaster) that cause many simultaneous fatalities than about the same number of fatalities occurring individually over time (Vrijling et al., 1998; Jonkman et al., 2008). In this study, societal risk describes the relationship between the frequency of hazardous events and the number of people affected, typically expressed through frequency–fatality relationships. However, in a broader interpretation the concept of societal risk may also encompass wider societal impacts, including the social and political responses that major disasters can generate (Stroud and McDougall, 2021). As highlighted in previous studies on risk in hazardous industries (Ball and Floyd, 1998), the term itself has often been a source of ambiguity, as it has been used to describe both the statistical relationship between event frequency and the number of affected individuals and, more broadly, the societal consequences that may follow major disasters. In the context of this work, our estimates should therefore be interpreted strictly as measures of societal risk in its probabilistic sense, rather than as comprehensive assessments of social risk.

5. Conclusions

In this work, we characterize societal flood risk in Italy by adopting a statistical approach in which the spatial distribution of the societal risk is determined based on historical, sparse data on flood fatalities covering a 78-year period 1946-september 2023. The Zipf distribution, was adopted to describe the frequency–magnitude relationship of fatal flood events. The geographical distribution of the Zipf variables (Fig. 5) highlight that the three Zipf parameters—E (number of fatal floods), F (largest recorded magnitude), and s (scaling exponent)— capture different facets of societal flood risk. Their combined interpretation provides a more comprehensive representation of the spatial variability of flood impacts on society. The analysis shows that the most probable magnitudes correspond to events with 3–7 fatalities while the spatial distribution of E is strongly skewed, with about 31% of the cells not exceeding 12 fatal events during the entire observation period. Nearly half of the national territory (48.02%) exhibits values of the Zipf exponent $s \leq 1.8$, indicating a prevalence of small-magnitude events, whereas areas with $s \leq 1$ indicate a relatively higher contribution of large-magnitude events. Based on these parameters, societal flood risk scenarios were derived for four increasing fatality thresholds ($f = 1, 3, 5, 10$) and represented through spatially distributed maps (Fig. 6). The approach estimates the likelihood of flood events of varying magnitudes in terms of number of fatalities (f). Starting from the probability mass function (PMF), we derived both the yearly complementary cumulative distribution function (yCCFDF), representing the annual frequency of fatal floods of a given magnitude, and the expected return period τ, describing the average recurrence interval between fatal floods of a given magnitude. For most of the Italian territory, the estimated return period is generally $\tau < 50$ years, indicating frequent occurrences of low-fatality flood events across the country, whereas high-magnitude fatal floods remain rare and spatially concentrated in specific physiographic regions.

The performance of the spatially distributed Zipf-based model was evaluated by comparing modelled scenarios, derived from the calibration period (1946–2010), with independent observational data spanning the validation period (2011–September 2023) (Fig. 7), across eight main morphological subdivisions of Italy.

The comparison indicates a general tendency for the modelled return periods to be slightly overestimated relative to those observed, with the exception of the Alpine Mountain System. This suggests that fatal floods have occurred more frequently in recent decades than predicted by the

long-term model.

Overall, the results indicate that while the model performs reliably under stationary assumptions, recent changes in flood occurrence highlight the need for periodic model recalibration and continuous data integration. These findings also emphasize the importance of further investigating the potential non-stationarity of extreme events in order to improve the predictive capacity of societal flood risk assessments.

Furthermore, the objective of this study is to provide a synoptic, homogeneous, and standardized framework for evaluating the risk that floods pose to the population. This objective can be achieved by applying the same methodological approach consistently across the entire territory. The resulting analysis can therefore offer valuable insights for identifying areas characterized by different levels of risk and for supporting the planning of mitigation strategies aimed at protecting the population.

Our work confirms the model's ability to accurately represent spatial patterns and recurrence scales of societal flood risk, revealing emerging signals of a recent increase in the frequency of impacts, highlighting the need for regular data updates and close integration between modelling, monitoring and risk reduction policies. Nevertheless, the combined use of scenarios and morphological comparisons makes it possible to clearly identify geographical areas on which to prioritise structural and non-structural prevention measures e.g. planning, warning systems, risk education and exposure management.

Funding

This research did not receive any specific grant from funding agencies in the public, commercial, or not-for-profit sectors.

CRediT authorship contribution statement

Paola Salvati: Conceptualization, Data curation, Methodology, Writing – original draft, Writing – review & editing. **Mina Yazdani:** Data curation, Formal analysis, Writing – original draft, Writing – review & editing. **Cinzia Bianchi:** Data curation, Visualization. **Mauro Rossi:** Formal analysis, Methodology, Supervision, Validation.

Declaration of competing interest

The authors declare that they have no known competing financial interests or personal relationships that could have appeared to influence the work reported in this paper.

Acknowledgments

M.Y. was supported by a grant awarded by the Italian National Research Council (CNR), project DTA. AD003.474 “Cambiamento climatico: mitigazione del rischio per uno sviluppo sostenibile (quota FOE Fondo Ordinario per gli Enti di Ricerca 2019)"

Appendix A. Supplementary data

Supplementary data to this article can be found online at https://doi.org/10.1016/j.jenvman.2026.129892.

Data availability

The data outputs are provided in the Supplementary Materials as an Excel file named calibration-model_data rew2

References

Australian Geomechanics Society AGS, 2007a. Guideline for landslide susceptibility, hazard and risk zoning for land use planning. Aust. Geomech. 42 (1), 13–36.
Australian Geomechanics Society, AGS, 2007b. Practice note guidelines for landslide risk management. https://landsliderisk.org/resources/guidelines/.
ANCOLD, Australian National Committee on Large Dams, 2003. Guidelines on Risk Assessment.
Arnell, N.W., Gosling, S.N., 2016. The impacts of climate change on river flood risk at the global scale. Clim. Change 134, 387–401. https://doi.org/10.1007/s10584-014-1084-5.
Arrighi, C., Domeneghetti, A., 2024. Brief communication: on the environmental impacts of the 2023 floods in Emilia-Romagna (italy). Nat. Hazards Earth Syst. Sci. 24, 673–679. https://doi.org/10.5194/nhess-24-673-2024.
Avino, A., Cimorelli, L., Furcolo, P., Noto, L.V., Pelosi, A., Pianese, D., Villani, P., Manfreda, S., 2024. Are rainfall extremes increasing in southern Italy? J. Hydrol. 631, 130684. https://doi.org/10.1016/j.jhydrol.2024.130684.
Baecher, G., Abedinisohi, F., Pate Baecher, R., 2015. Societal Risk Criteria for Loss of Life: Concepts, History, and Mathematics. University of Maryland, College Park, MD.
Ball, D.J., Floyd, P.J., 1998. Societal Risks – a Report Prepared for the Health and Safety Executive.
Birkmann, J., 2007. Risk and vulnerability indicators at different scales: applicability, usefulness and policy implications. Environ. Hazards 7 (1), 20–31. https://doi.org/10.1016/j.envhaz.2007.04.002. ISSN 1747-7891.
Blöschl, G., 2022. Flood generation: process patterns from the raindrop to the ocean. Hydrol. Earth Syst. Sci. 26, 2469–2480. https://doi.org/10.5194/hess-26-2469-2022.
Brunetti, M., Colacino, M., Maugeri, M., Nanni, T., 2001. Trends in the daily intensity of precipitation in Italy from 1951 to 1996. Int. J. Climatol. 21, 299–316. https://doi.org/10.1002/joc.613.
Brunetti, M., Maugeri, M., Monti, F., Nanni, T., 2004. Changes in daily precipitation frequency and distribution in Italy over the last 120 years. J. Geophys. Res. 109, D05102. https://doi.org/10.1029/2003JD004296.
Caporali, E., Lompi, M., Pacetti, T., Chiarello, V., Fatichi, S., 2021. A review of studies on observed precipitation trends in Italy. Int. J. Climatol. 41, E1–E25. https://doi.org/10.1002/joc.6741.
Ciurean, R.L., Schroter, D., Glade, T., 2013. Conceptual frameworks of vulnerability assessments for natural disasters reduction. In: Tiefenbacher, J. (Ed.), Approaches to Disaster Management - Examining the Implications of Hazards, Emergencies and Disasters. InTech. https://doi.org/10.5772/55538.
Clauset, A., Shalizi, C.R., Newman, M.E.J., 2009. Power-law distributions in empirical data. SIAM Rev. 51, 661–703. https://doi.org/10.1137/070710111.
Centre for Research on the Epidemiology of Disasters, 2021. 2020: the Non-COVID Year in Disasters: Global Trends and Perspectives. Centre for Research on the Epidemiology of Disasters (CRED), Brussels. https://emdat.be/sites/default/files/adsr_2020.pdf.
Cremonini, L., Randi, P., Fazzini, M., Nardino, M., Rossi, F., Georgiadis, T., 2024. Causes and impacts of flood events in Emilia-Romagna (Italy) in May 2023. Land 13, 1800. https://doi.org/10.3390/land13111800.
Cruden, D.M., 1997. Estimating the risk from landslides using historical data. In: Cruden, D.M., Fell, R. (Eds.), Landslide Risk Assessment. Balkema, Rotterdam, pp. 177–184.
Davison, A.C., Hinkley, D.V., 1997. Bootstrap Methods and their Application. Cambridge University Press, Cambridge. https://doi.org/10.1017/CBO9780511802843.
De Bruijn, K.M., Diermanse, F.L.M., Beckers, J.V.L., 2014. An advanced method for flood risk analysis in river deltas, applied to societal flood fatality risk in the Netherlands. Nat. Hazards Earth Syst. Sci. 14, 2767–2781. https://doi.org/10.5194/nhess-14-2767-2014.
Diakakis, M., Papagiannaki, K., 2021. Characteristics of indoor flood fatalities: evidence from Greece. Sustainability 13, 8612. https://doi.org/10.3390/su13158612.
European Environment Agency (EEA), 2000. CORINE Land Cover 2000 (CLC2000). Copernicus Land Monitoring Service.
Efron, B., 1979. Bootstrap methods: another look at the jackknife. Ann. Stat. 7, 1–26. https://doi.org/10.1214/aos/1176344552.
EU – European Union, 2007. Directive 2007/60/EC of the european parliament and of the council of 23 October 2007 on the assessment and management of flood risks. Off. J. Eur. Union L288, 27–34.
Evans, A.W., Verlander, N.Q., 1997. What is wrong with criterion FN-Lines for judging the tolerability of risk? Risk Anal. 17, 157–168. https://doi.org/10.1111/j.1539-6924.1997.tb00855.x.
Falcucci, A., Maiorano, L., Boitani, L., 2006. Changes in land-use/land-cover patterns in Italy and their implications for biodiversity conservation. Landsc. Ecol. 22, 617–631. https://doi.org/10.1007/s10980-006-9056-4.
Federal Energy Regulatory Commission, 2016. *Risk-Informed Decision Making (RIDM): Risk Guidelines for Dam Safety* (Interim Guidance. Version 4.1.
Fell, R., Ho, K.K.S., Lacasse, S., Leroi, E., 2005. A framework for landslide risk assessment and management. In: Hungr, O., Fell, R., Couture, R., Eberhardt, E. (Eds.), Landslide Risk Management. Taylor & Francis, pp. 3–26.
Fell, R., Hartford, D., 1997. Landslide risk management. In: Cruden, D.M., Fell, R. (Eds.), Proceedings of the International Workshop on Landslide Risk Assessment, Honolulu, Hawaii, 19–21 February 1997. Balkema, Rotterdam, pp. 51–109.
Friedman, J.A., 2015. Using power laws to estimate conflict size. J. Conflict Resolut. 59, 1216–1241. https://doi.org/10.1177/0022002714530430.
Gariano, S.L., Guzzetti, F., 2016. Landslides in a changing climate. Earth Sci. Rev. 162, 227–252. https://doi.org/10.1016/j.earscirev.2016.08.011.
Guzzetti, F., Stark, C.P., Salvati, P., 2005. Evaluation of flood and landslide risk to the population of Italy. Environ. Manag. 36 (1), 15–36. https://doi.org/10.1007/s00267-003-0257-1.
Guzzetti, F., Reichenbach, P., 1994. Towards a definition of topographic divisions for Italy. Geomorphology 11, 57–74. https://doi.org/10.1016/0169-555X(94)90042-6.

Hamilton, K., Demant, D., Peden, A.E., Hagger, M.S., 2020. A systematic review of human behaviour in and around floodwater. Int. J. Disaster Risk Reduct. 47, 101561. https://doi.org/10.1016/j.ijdrr.2020.101561.
Health and Safety Executive (HSE), 2001. Reducing Risks, Protecting People: HSE Decision-Making Process. HSE, United Kingdom.
Hosseinzadehtalaei, P., Tabari, H., Willems, P., 2020. Climate change impact on short-duration extreme precipitation and intensity–duration–frequency curves over Europe. J. Hydrol. 590, 125249. https://doi.org/10.1016/j.jhydrol.2020.125249.
Jongejan, R.B., Jonkman, S.N., Maaskant, B., 2010. The potential use of individual and societal risk criteria within the Dutch flood safety policy (part 1): basic principles. In: Briš, R., Guedes Soares, C., Martorell, S. (Eds.), Reliability, Risk and Safety: Theory and Applications. Taylor & Francis Group, London, pp. 1773–1780.
Jonkman, S.N., Curran, A., Bouwer, L.M., 2024. Floods have become less deadly: an analysis of global flood fatalities 1975–2022. Nat. Hazards 120, 6327–6342. https://doi.org/10.1007/s11069-024-06444-0.
Jonkman, S.N., Jongejan, R., Maaskant, B., 2011. The use of individual and societal risk criteria within the Dutch flood safety policy—nationwide estimates of societal risk and policy applications. Risk Anal. 31, 282–300. https://doi.org/10.1111/j.1539-6924.2010.01502.x.
Jonkman, S.N., Kok, M., Vrijling, J.K., 2008. Flood risk assessment in The Netherlands: a case study for dike ring South Holland. Risk Anal 28 (5), 1357–1374. https://doi.org/10.1111/j.1539-6924.2008.01103.x. Epub 2008 Aug 21. PMID: 18761731.
Jonkman, S.N., Maaskant, B., Kolen, B., Needham, J.T., 2016. Loss of life estimation—review, developments and challenges. In: Lang, M., Klijn, F., Samuels, P. (Eds.), 3rd European Conference on Flood Risk Management. EDP Sciences. https://doi.org/10.1051/e3sconf/20160706004.
Kahraman, A., Kendon, E.J., Chan, S.C., Fowler, H.J., 2021. Quasi-stationary intense rainstorms spread across Europe under climate change. Geophys. Res. Lett. 48. https://doi.org/10.1029/2020GL092361 e2020GL092361.
Kley, T., Preuß, P., Fryzlewicz, P., 2019. Predictive finite-sample model choice for time series under stationarity and non-stationarity. Electron. J. Stat. 13 (2), 3710–3774. https://doi.org/10.1214/19-EJS1606.
Kundzewicz, Z.W., Su, B., Wang, Y., Wang, G., Wang, G., Huang, J., Jiang, T., 2019. Flood risk in a range of spatial perspectives – from global to local scales. Nat. Hazards Earth Syst. Sci. 19, 1319–1328. https://doi.org/10.5194/nhess-19-1319-2019.
Li, C., Sun, N., Lu, Y., Guo, B., Wang, Y., Sun, X., Yao, Y., 2023. Review on urban flood risk assessment. Sustainability 15, 765. https://doi.org/10.3390/su15010765.
Maaskant, B., Jonkman, S.N., Jongejan, R.B., 2010. The potential use of individual and societal risk criteria within the Dutch flood safety policy (part 2): estimation of the individual and societal risk for the dike rings in the Netherlands. In: Briš, R., Guedes Soares, C., Martorell, S. (Eds.), Reliability, Risk and Safety: Theory and Applications. Taylor & Francis Group, London, pp. 1781–1788.
Macciotta, R., Gräpel, C., Keegan, T., Duxbury, J., Skirrow, R., 2019. Quantitative risk assessment of rock slope instabilities that threaten a highway near Canmore, Alberta, Canada: managing risk calculation uncertainty in practice. Can. Geotech. J. 57, 337–353.
Macciotta, R., Lefsrud, L., 2018. Framework for developing risk to life evaluation criteria associated with landslides in Canada. Geoenvironmental Disasters 5, 10.
Marchesini, I., Salvati, P., Rossi, M., Donnini, M., Sterlacchini, S., Guzzetti, F., 2021. Data-driven flood hazard zonation of Italy. J. Environ. Manag. 294, 112986. https://doi.org/10.1016/j.jenvman.2021.112986.
Merz, B., Aerts, J.C.J.H., Arnbjerg-Nielsen, K., Baldi, M., Becker, A., Bichet, A., Blöschl, G., Bouwer, L.M., Brauer, A., Cioffi, F., Delgado, J.M., Gocht, M., Guzzetti, F., Harrigan, S., Hirschboeck, K., Kilsby, C., Kron, W., Kwon, H.-H., Lall, U., Merz, R., Nissen, K., Salvati, P., Swierczynski, T., Ulbrich, U., Viglione, A., Ward, P. J., Weiler, M., Wilhelm, B., Nied, M., 2014. Floods and climate: emerging perspectives for flood risk assessment and management. Nat. Hazards Earth Syst. Sci. 14, 1921–1942. https://doi.org/10.5194/nhess-14-1921-2014.
Merz, B., Blöschl, G., Vorogushyn, S., et al., 2021. Causes, impacts and patterns of disastrous river floods. Nat. Rev. Earth Environ. 2, 592–609. https://doi.org/10.1038/s43017-021-00195-3.
Merz, B., Hall, J., Disse, M., Schumann, A., 2010. Fluvial flood risk management in a changing world. Nat. Hazards Earth Syst. Sci. 10, 509–527. https://doi.org/10.5194/nhess-10-509-2010.
Newman, M.E.J., 2005. Power laws, pareto distributions and Zipf's law. Contemp. Phys. 46, 323–351.
Papagiannaki, K., et al., 2022. Developing a large-scale dataset of flood fatalities. Sci. Data 9, 166. https://doi.org/10.1038/s41597-022-01273-x.
Pendergrass, A.G., Knutti, R., Lehner, F., Deser, C., Sanderson, B.M., 2017. Precipitation variability increases in a warmer climate. Sci. Rep. 7, 17966. https://doi.org/10.1038/s41598-017-17966-y.
Petrucci, O., 2022. Factors leading to flood fatalities: a systematic review of research papers published between 2010 and 2020. Nat. Hazards Earth Syst. Sci. 22, 71–83. https://doi.org/10.5194/nhess-22-71-2022.
Porter, M., Morgenstern, N., 2013. Landslide Risk Evaluation – Canadian Technical Guidelines and Best Practices Related to Landslides: a National Initiative for Loss Reduction. Geological Survey of Canada. https://doi.org/10.4095/292234. Open File 7312.
Reed, W.J., 2001. The pareto, zipf and other power laws. Econ. Lett. 74, 15–19. https://doi.org/10.1016/S0165-1765(01)00524-9.
Reid, S.G., 2000. Acceptable risk criteria. Prog. Struct. Engng Mater. 2, 254–262. https://doi.org/10.1002/1528-2716(200004/06)2:2<254::AID-PSE30>3.0.CO;2-K.
Rossi, M., Guzzetti, F., Salvati, P., Donnini, M., Napolitano, E., Bianchi, C., 2019. A predictive model of societal landslide risk in Italy. Earth Sci. Rev. 196, 102849. https://doi.org/10.1016/j.earscirev.2019.04.021.
Rossi, M., Witt, A., Guzzetti, F., Malamud, B.D., Peruccacci, S., 2010. Analysis of historical landslide time series in the Emilia-Romagna region, northern Italy. Earth Surf. Process. Landf. 35, 1123–1137. https://doi.org/10.1002/esp.1858.
Ryan, O., Haslbeck, J.M.B., Waldorp, L.J., 2025. Non-stationarity in time-series analysis: modeling stochastic and deterministic trends. Multivariate Behav. Res. 60, 556–588. https://doi.org/10.1080/00273171.2024.2436413.
Salvati, P., Bianchi, C., Rossi, M., Guzzetti, F., 2010. Societal landslide and flood risk in Italy. Nat. Hazards Earth Syst. Sci. 10, 465–483. https://doi.org/10.5194/nhess-10-465-2010.
Salvati, P., Bianchi, C., Rossi, M., Guzzetti, F., 2012. Flood risk in Italy. In: Kundzewicz, Z.W. (Ed.), Changes in Flood Risk in Europe. IAHS, pp. 277–292.
Salvati, P., Petrucci, O., Rossi, M., Bianchi, C., Pasqua, A.A., Guzzetti, F., 2018. Gender, age and circumstances analysis of flood and landslide fatalities in Italy. Sci. Total Environ. 610–611, 867–879. https://doi.org/10.1016/j.scitotenv.2017.08.064.
Saw, J.L., Wardman, M., Wilday, J., 2009. Societal risk: initial briefing to the societal risk technical advisory group (Research Report RR703). Health and Safety Executive, Sudbury, UK.
Schanze, J., Zeman, E., Marsalek, J. (Eds.), 2007. Flood Risk Management: Hazards, Vulnerability and Mitigation Measures. Springer, Dordrecht.
Sim, K.B., Lee, M.L., Wong, S.Y., 2022. A review of landslide acceptable risk and tolerable risk. Geoenviron. Disasters 9, 3. https://doi.org/10.1186/s40677-022-00205-6.
Strouth, A., McDougall, S., 2021. Societal risk evaluation for landslides: historical synthesis and proposed tools. Landslides 18, 1071–1085. https://doi.org/10.1007/s10346-020-01547-8.
Strouth, A., McDougall, S., 2022. Individual risk evaluation for landslides: key details. Landslides 19, 939–955. https://doi.org/10.1007/s10346-021-01838-8.
Sui, H., Hu, R., Gao, W., Gao, W., Luo, G., 2020. Risk assessment of individual landslide based on the risk acceptable model: a case study of the Shiyantan landslide in Mayang County, China. Hum. Ecol. Risk Assess. 26 (9), 2500–2519. https://doi.org/10.1080/10807039.2019.1710461.
Tabari, H., 2020. Climate change impact on flood and extreme precipitation increases with water availability. Sci. Rep. 10, 13768. https://doi.org/10.1038/s41598-020-70816-2.
Tabasi, N., Fereshtehpour, M., Roghani, B., 2025. A review of flood risk assessment frameworks and the development of hierarchical structures for risk components. Discov. Water 5, 10. https://doi.org/10.1007/s43832-025-00193-2.
Tang, Y., Zhang, X., Chen, W., 2021. Scenario-based economic and societal risk assessment of storm flooding in Shanghai. Int. J. Clim. Change Strateg. Manag. 13 (4/5), 529–546. https://doi.org/10.1108/IJCCSM-05-2020-0051.
UNISDR, 2015. Sendai framework for disaster risk reduction 2015–2030. https://www.unisdr.org/we/inform/publications/43291.
USBR, 2003. Reclamation. Guidelines for Achieving Public Protection in Dam Safety Decision Making. U.S. Bureau of Reclamation, Denver, Colorado.
USBR, 2011. Reclamation. *Dam safety public protection guidelines: a risk framework to support dam safety decision-making (Interim)*. In: US Department of the Interior, Bureau of Reclamation, Dam Safety Office, Denver, CO. August 2011.
Vrijling, J.K., van Hengel, W., Houben, R.J., 1998. Acceptable risk as a basis for design. Reliab. Eng. Syst. Saf. 59, 1–13. https://doi.org/10.1016/S0951-8320(97)00135-X.
Wang, L., Cui, S., Li, Y., Huang, H., Manandhar, B., Nitivattananon, V., Fang, X., Huang, W., 2022. A review of flood management: from flood control to flood resilience. Heliyon 8, e11763. https://doi.org/10.1016/j.heliyon.2022.e11763.
Wasko, C., Sharma, A., 2017. Global assessment of flood and storm extremes with increased temperatures. Sci. Rep. 7, 7945. https://doi.org/10.1038/s41598-017-08481-1.
White, E.P., Enquist, B.J., Green, J.L., 2008. On estimating the exponent of power-law distributions. Ecology 89, 905–912. https://doi.org/10.1890/07-1288.1.
Wing, O.E., Bates, P.D., Smith, A.M., Sampson, C.C., Johnson, K.A., Fargione, J., Morefield, P., 2018. Estimates of present and future flood risk in the conterminous United States. Environ. Res. Lett. 13, 034023.
Winsemius, H.C., Van Beek, L.P.H., Jongman, B., Ward, P.J., Bouwman, A., 2013. A framework for global river flood risk assessments. Hydrol. Earth Syst. Sci. 17, 1871–1892. https://doi.org/10.5194/hess-17-1871-2013.
Winter, M.G., Wong, J.C.F., 2020. The assessment of quantitative risk to road users from debris flow. Geoenviron. Disasters 7, 4. https://doi.org/10.1186/s40677-019-0140-x.
Zhang, J., Xu, W., Liao, X., Zong, S., Liu, B., 2021. Global mortality risk assessment from river flooding under climate change. Environ. Res. Lett. 16 (6), 064012. https://doi.org/10.1088/1748-9326/abff87.
Zipf, G.K., 1949. Human Behavior and the Principle of Least Effort. Addison-Wesley Press, Cambridge.

Further reading

UNDRR, 2017. The Sendai Framework Terminology on Disaster Risk Reduction. Hazard. https://www.undrr.org/terminology/hazard.
Zielinski, P.A., Baecher, G.B., 2012. Comparative Analysis of Technological and Intelligent Terrorism Impacts on Complex Technical Systems. In: Makhutov, N.A., Baecher, G.B. (Eds.), NATO Science for Peace and Security Series E: Human and Societal Dynamics, 102. IOS Press, Amsterdam, pp. 168–183.